Geomorphology 321 (2018) 146–152

Contents lists available at ScienceDirect

Geomorphology

journal homepage: www.elsevier.com/locate/geomorph

A Lagrangian framework for exploring complexities of mixed-size sediment transport in gravel-bedded river networks

Jonathan A. Czuba

Department of Biological Systems Engineering, Virginia Tech, Seitz Hall, 155 Ag Quad Lane, Blacksburg, VA 24061, USA

ARTICLE INFO

Article history:
Received 1 February 2018
Received in revised form 22 August 2018
Accepted 22 August 2018
Available online 24 August 2018

Keywords:
River network
Sediment mixture
Complexity
Gravel-bedded river
Sediment transport
Network model

ABSTRACT

The movement of sediment from source to sink in a watershed is a complex process with multiple interactions and feedbacks across scales. At small scales, the size characteristics of a sediment mixture affect the transport of that sediment through hiding and through the nonlinear effect of sand content on gravel transport. At large scales, the channel network itself, through network geometry and the spatial pattern of transport capacity, adds additional complexity in organizing sediment moving through the system such that aggradational hotspots can emerge. The purpose of this paper is to present a Lagrangian framework for exploring complexities of mixed-size sediment transport in gravel-bedded river networks. The present model builds off of previous network-based, bed-material sediment transport models; but key advancements presented herein (i) allow for a mixture of sediment sizes in the river network, (ii) incorporate a mixed-size sediment transport equation, and (iii) utilize a daily flow hydrograph to drive intermittent transport. The model is applied to the roughly 4700 km^2 Methow River Basin in Washington State, USA, using simplified model inputs with the goal of illustrating the utility of the model for motivating future work.

1. Introduction

The movement of sediment from source to sink in a watershed is a complex process with multiple interactions and feedbacks across scales. For example, the sediment size distribution supplied by hillslopes to channels depends on lithology, climate, life, erosion rate, and topography (Sklar et al., 2017). Furthermore, the frequency-magnitude characteristics of the sediment supply are inherently stochastic because of rainstorms, topography, colluvial properties, and recovery from past events (Benda and Dunne, 1997b). Once emplaced, spatially variable, local channel properties transform the flow of water into a driving force for moving sediment downstream. Mixing, hiding, and grain-size specific transport of sediment affect how an individual rock moves downstream (Parker, 2008). This already complex transport process is further confounded by additional granular interactions that lead to imbrication, armoring, patch formation, and the creation of force chains (Frey and Church, 2011) as well as stress history, which results in vertical settlement, changes in roughness, particle repositioning, and changes in the entrainment threshold (Ockelford and Haynes, 2013). At larger scales, the channel network itself, through network geometry and the spatial pattern of transport capacity, adds additional complexity in organizing sediment moving through the system such that aggradational hotspots can emerge (Benda et al., 2004; Czuba and Foufoula-Georgiou, 2015; Czuba et al., 2017; Gran and Czuba, 2017; Rice, 2017; Schmitt et al., 2018; Walley et al., 2018).

Incorporating all of these process dynamics across multiple scales into a single modeling framework seems computationally prohibitive at present. Instead, exploring a subset of this complexity is common based on a scale or component of interest. Herein, the interest is in exploring mixed-size sediment transport on a river network. Relevant to this scope, one dimensional (1D) sediment transport models have been developed that incorporate mixed-size sediment dynamics. The Unified Gravel-Sand (TUGS) model incorporates transport dynamics of a sand-gravel grain size distribution via a surface-based bedload equation, three conceptual layers (bedload, surface, and subsurface), transfer functions between layers, and abrasion (Cui, 2007). The Morphodynamics and Sediment Tracers in 1D (MAST-1D) model also incorporates mixed-size transport, but its key contribution is in its handling of size-specific exchange between sediment in the channel and floodplain (Lauer et al., 2016). However, these 1D models cannot suitably explore additional complexities that arise from channel network structure.

River network models have been created to explicitly explore network structure, although they have not yet sufficiently advanced to incorporate the dynamic processes of their 1D model counterparts (e.g., TUGS, MAST-1D). One major shortcoming of existing river network models is that they do not incorporate physically based dynamics of mixed-sized sediment transport (Benda and Dunne, 1997a; Jacobson and Gran, 1999; Wilkinson et al., 2006; Czuba and Foufoula-Georgiou,

E-mail address: jczuba@vt.edu.

https://doi.org/10.1016/j.geomorph.2018.08.031
0169-555X/

2014, 2015; Schmitt et al., 2016; Czuba et al., 2017; Gran and Czuba, 2017; Schmitt et al., 2018). It remains to be seen how multiple size fractions interact during transport on river networks (e.g., via the incorporation of a mixed-size sediment transport equation such as Wilcock and Crowe, 2003).

The purpose of this paper is to present a Lagrangian framework for exploring complexities of mixed-size sediment transport in gravel-bedded river networks. The present model builds off of previous work by Czuba and Foufoula-Georgiou (2014, 2015), Czuba et al. (2017), and Gran and Czuba (2017), but key advancements herein allow for a mixture of sediment sizes in the river network, incorporate the mixed-size sediment transport equation of Wilcock and Crowe (2003), and utilize a daily flow hydrograph to drive intermittent transport. The model is applied to the roughly 4700 km^2 Methow River Basin in Washington State, USA, using simplified model inputs. The goal is to illustrate the utility of the model for motivating future work rather than to provide a detailed case study for the Methow River Basin.

2. Network-based modeling framework for mixed-size sediment

2.1. Network of river channels

The basis of the model is a river network that is conceptualized as a set of connected links. Each link i represents a segment of river channel with a set of unique, and possibly time-variable, topologic, physical, and hydrodynamic attributes. The spatial extent of a link is between tributaries (so attributes of a link remain constant throughout the length of a link) and no longer than a given length. That is, long reaches between tributaries can be broken into multiple links to ensure an upper limit to the maximum link length.

2.2. Sediment conceptualization

Sediment is conceptualized in the model as discrete units referred to as parcels p. An individual parcel represents an arbitrary volume of sediment that moves downstream as a coherent unit. Each parcel has a set of unique geometric, sedimentologic, and lithologic attributes including: volume V_p [L^3] and grain size d_p [L]. The model is capable of allowing parcel volume and parcel grain size to vary in time as sediment is broken down via attrition, but these dynamics are not incorporated in the present model. The spatiotemporal distribution of sediment parcels input to the network will depend on the specific basin under study. The model itself is flexible enough to allow for sediment parcel input anywhere along the length of a link and at any point in time.

2.3. Two-layer model

At any time t [T] multiple parcels can be present with different volumes and grain sizes within a given link i. The total parcel volume in each link i at time t or $V_{i,t}$ [L^3] is the sum of the volumes of all parcels within that link at that particular time given as

$$V_{i,t} = \sum_{\substack{\text{all parcels } p \\ \text{in link } i \\ \text{at time } t}} V_p \tag{1}$$

The total volume of sediment in a link is separated into an active/surface layer and a storage/subsurface layer (see Czuba et al., 2017). The volume of sediment in the active/surface layer at transport capacity $\chi_{i,t}$ [L^3] is given by

$$\chi_{i,t} = \ell_i B_{i,t} L_{a,i,t} \tag{2}$$

where ℓ_i [L] is the length, $B_{i,t}$ [L] is the channel width, and $L_{a,i,t}$ [L] is the active layer thickness in link i. Thus, the total parcel volume in the active/surface layer of link i at time t or $V_{i,t}^{act}$ [L^3] is given by

$$V_{i,t}^{act} = \begin{cases} \chi_{i,t}, & \text{for } V_{i,t} > \chi_{i,t} \\ V_{i,t}, & \text{for } V_{i,t} \le \chi_{i,t} \end{cases} \tag{3}$$

Any volume of sediment within a link beyond what can be moved at capacity is placed in the storage/subsurface layer, is not transported at that time, and acts to increase the slope in the link and decrease the slope(s) in the immediately upstream link(s) (see Czuba et al., 2017, for further details). The order of arrival of parcels is preserved in the model and each parcel is tracked as it moves through a link. Following first-in, last-out, the last parcels to arrive to a link and whose cumulative volume is $\le \chi_{i,t}$ are placed in the active/surface layer.

The active/surface layer and storage/subsurface layer are only formed if enough parcels reside in that link. When no parcels are within a link, nothing is transported, and the link is treated as bedrock floored. As a few parcels enter a link (whose total volume within the link is less than the volume transported at capacity), the link is still treated as bedrock floored, no storage/subsurface layer exists, and all the parcels within the link are within the active layer. When more parcels than can be moved at capacity reside in a link, only then does the storage/subsurface layer exist. In this Lagrangian framework, bed elevation is computed from the total number of parcels over the link surface area (length times width), including porosity (see Czuba et al., 2017, for further details). Thus, as parcels enter and exit a link, the bed elevation is updated accordingly.

2.4. Mixed-size sediment transport

2.4.1. Sedimentologic characteristics of a link

The transport calculation begins by first computing the sedimentologic characteristics of a link at a particular time from the parcels within that link. Within the active/surface layer of link i at time t, the mean size of the bed surface sediment $d_{i,t}$ [L] (including sand and gravel grain size classes) is computed as

$$d_{i,t} = \frac{1}{V_{i,t}^{act}} \sum_{\substack{\text{all parcels } p \\ \text{in active layer} \\ \text{of link } i \\ \text{at time } t}} d_p V_p \tag{4}$$

The fraction of sand in the active/surface layer of link i at time t or $F_{s,i,t}$ is computed as

$$F_{s,i,t} = \frac{1}{V_{i,t}^{act}} \sum_{\substack{\text{sand parcels } p \\ \text{in active layer} \\ \text{of link } i \\ \text{at time } t}} V_p \tag{5}$$

and the fraction of parcel p in the active/surface layer of link i at time t or $F_{p,i,t}$ is computed as

$$F_{p,i,t} = \frac{V_p}{V_{i,t}^{act}} \tag{6}$$

2.4.2. Surface-based transport equation of Wilcock and Crowe (2003)

The transport of mixed-size sediment follows the surface-based, bedload equation of Wilcock and Crowe (2003). Under this

formulation, the dimensionless transport rate for parcel p or $W^*_{p,i,t}$ is given by

$$W^*_{p,i,t} = \begin{cases} 0.002\left(\frac{\tau_{i,t}}{\tau_{rp,i,t}}\right)^{7.5}, & \text{for } \frac{\tau_{i,t}}{\tau_{rp,i,t}} < 1.35 \\ 14\left(1-\frac{0.894}{\sqrt{\frac{\tau_{i,t}}{\tau_{rp,i,t}}}}\right)^{4.5}, & \text{for } \frac{\tau_{i,t}}{\tau_{rp,i,t}} \geq 1.35 \end{cases} \quad (7)$$

where $\tau_{i,t}$ [$ML^{-1}T^{-2}$] is the bed shear stress (which can be computed in a number of ways, see Section 3.2.2 for this application), and $\tau_{rp,i,t}$ [$ML^{-1}T^{-2}$] is the reference shear stress for parcel p in link i at time t as

$$\tau_{rp,i,t} = \tau_{rm,i,t}\left(\frac{d_p}{d_{i,t}}\right)^b \quad (8)$$

where $\tau_{rm,i,t}$ [$ML^{-1}T^{-2}$] is the reference shear stress for the mean size of the bed surface sediment in link i at time t as

$$\tau_{rm,i,t} = \rho g R d_{i,t}\left(0.021 + 0.015e^{-20F_{s,i,t}}\right) \quad (9)$$

where ρ [ML^{-3}] is the density of water, g [LT^{-2}] is the acceleration due to gravity, and R is the submerged specific gravity of sediment; and b is an exponent given as

$$b = \frac{0.67}{1+e^{\left(1.5-\frac{d_p}{d_{i,t}}\right)}} \quad (10)$$

Finally, the travel time of a sediment parcel p to move through a link i at a particular time t in the absence of storage (an additional storage delay occurs because of inactive transport when the parcel is in the storage/subsurface layer, see Section 2.3 and Czuba et al., 2017) is given by dimensionalizing $W^*_{p,i,t}$ (see Wilcock and Crowe, 2003) and converting a volumetric transport rate into a transport time $t_{p,i,t}$ [T] through a link of length ℓ_i (see Czuba and Foufoula-Georgiou, 2014) as

$$t_{p,i,t} = \frac{\rho^{3/2} g R \ell_i L_{a,i,t}}{W^*_{p,i,t}\tau_{i,t}^{3/2} F_{p,i,t}} \quad (11)$$

3. Application to the Methow River Basin

3.1. Overview of the basin

The Methow River Basin covers roughly 4700 km^2 of primarily forest in north-central Washington State, USA (Fig. 1). The present model was applied to this river network because the network is self-similar (Zanardo et al., 2013) without large-scale geologic or anthropogenic features that strongly affect sediment transport (e.g., dams). The Methow River is a tributary to the Columbia River, which drains to the Pacific Ocean. Most precipitation falls as snow at high elevations in the winter months and snowmelt runoff leads to high streamflow during May and June (Mastin, 2015).

The average sediment particle size is between 0.04 and 0.14 m along the major river channels within the basin (Bureau of Reclamation, 2008; Anchor QEA, 2011). Larger sediment sizes are present in reaches with steeper slopes and this sediment could be reworked during 2-year peak flows (Bureau of Reclamation, 2008). However, the major river channels are relatively stable with no detectable trends of channel bed incision or aggradation on a decadal timescale (Bureau of Reclamation, 2008).

3.2. Model parameterization

3.2.1. Methow River network

The Methow River network was obtained from the National Hydrography Dataset Plus Version 2 (NHDPlusV2; McKay et al., 2012; Horizon

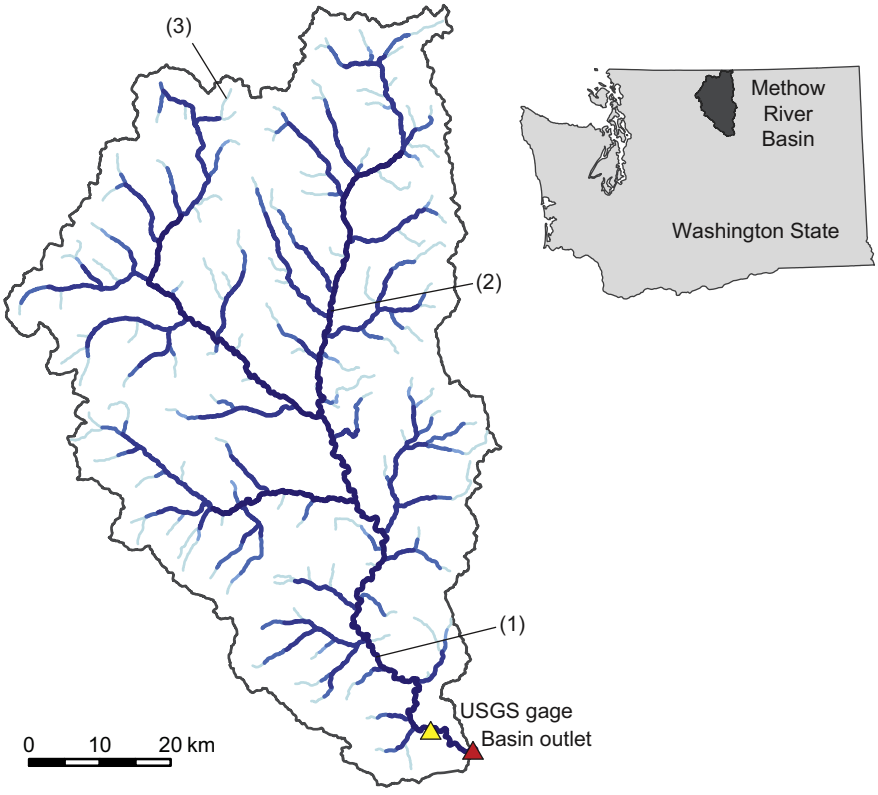

Fig. 1. Study area map of the Methow River Basin in Washington State, USA. Numbers (1)–(3) locate links for which data is shown in Fig. 2. The U.S. Geological Survey (USGS) gage is the Methow River near Pateros, WA, 12449950.

Systems, 2018). In preparing the NHDPlusV2 network for modeling, (i) the network was clipped to the extent of the Methow River Basin, (ii) isolated and secondary channels were removed, (iii) only links of the network with upstream drainage area >10 km^2 were retained, (iv) a new set of links was established between tributaries and no longer than 2 km, and (v) attributes for each link were recomputed from the original NHDPlusV2 data set. The final network was composed of 720 channel links each with attributes: index of link i, index of downstream link, link length ℓ_i, upstream drainage area A_i [L^2], elevation of the bed at the upstream end of the link $\eta_{i,t}$ [L], and channel slope $S_{i,t}$. A minimum channel slope of 1×10^{-3} was imposed in the model to avoid artificially low slopes from digital elevation model processing of backwater areas. This information forms the basis of the model and allows for the determination of the network topology.

3.2.2. Streamflow and channel hydraulic properties

Streamflow discharge and related hydraulic properties of flow depth, width, and velocity can be computed in a variety of ways for an entire river network. Herein, hydraulic properties of flow depth and width were scaled from the flow data at the U.S. Geological Survey (USGS) streamflow-gaging station nearest the basin outlet (Methow River near Pateros, WA, 12449950; USGS (2018)). First, based on field measurements at the gage (indicated by a subscript g), best-fit, at-a-station hydraulic geometry relations were developed between flow discharge $Q_{g,t}$ [L^3 T^{-1}] and both flow depth $H_{g,t}$ [L] and width $B_{g,t}$ [L] as

$$H_{g,t} = 0.27 Q_{g,t}^{0.34} \tag{12}$$

where $Q_{g,t}$ is specified in m^3 s^{-1} and $H_{g,t}$ in m ($n = 470$, $R^2 = 0.85$) and

$$B_{g,t} = 31 Q_{g,t}^{0.12} \tag{13}$$

where $Q_{g,t}$ is specified in m^3 s^{-1} and $B_{g,t}$ in m ($n = 470$, $R^2 = 0.44$).

Next, flow depth $H_{i,t}$ [L] and width $B_{i,t}$ throughout the entire network was scaled based on the conditions at the gage using typical exponents for downstream hydraulic geometry scaling (Leopold and Maddock Jr., 1953; Park, 1977) as

$$H_{i,t} = \left(\frac{H_{g,t}}{A_g^{0.4}}\right) A_i^{0.4} \tag{14}$$

and

$$B_{i,t} = \left(\frac{B_{g,t}}{A_g^{0.5}}\right) A_i^{0.5} \tag{15}$$

where A_g is the upstream drainage area at the gage.

Finally, the daily flow hydrograph at the gage $Q_{g,t}$ was used to compute $H_{g,t}$ and $B_{g,t}$ via Eqs. (12) and (13) respectively, which in turn were scaled to all links of the network to compute $H_{i,t}$ and $B_{i,t}$ via Eqs. (14) and (15) respectively. Thus, from a time-varying flow series at the gage, the above equations assign time-varying hydraulic properties (depth and width) throughout the entire river network. The key driver of sediment transport is shear stress $\tau_{i,t}$, which was computed using the depth-slope product as

$$\tau_{i,t} = \rho g H_{i,t} S_{i,t} \tag{16}$$

Specific parameter values assigned in the model included: $\rho = 1000$ kgm^{-3}, $g = 9.81$ ms^{-2}, and $R = 1.65$. The flow data at the gage used in the model simulation was for a 5-year period starting in water year (WY) 1970 and through WY 1974 (Fig. 2A). The peak flow in WY 1972 was the highest flow in the 58-year daily flow record at the gage.

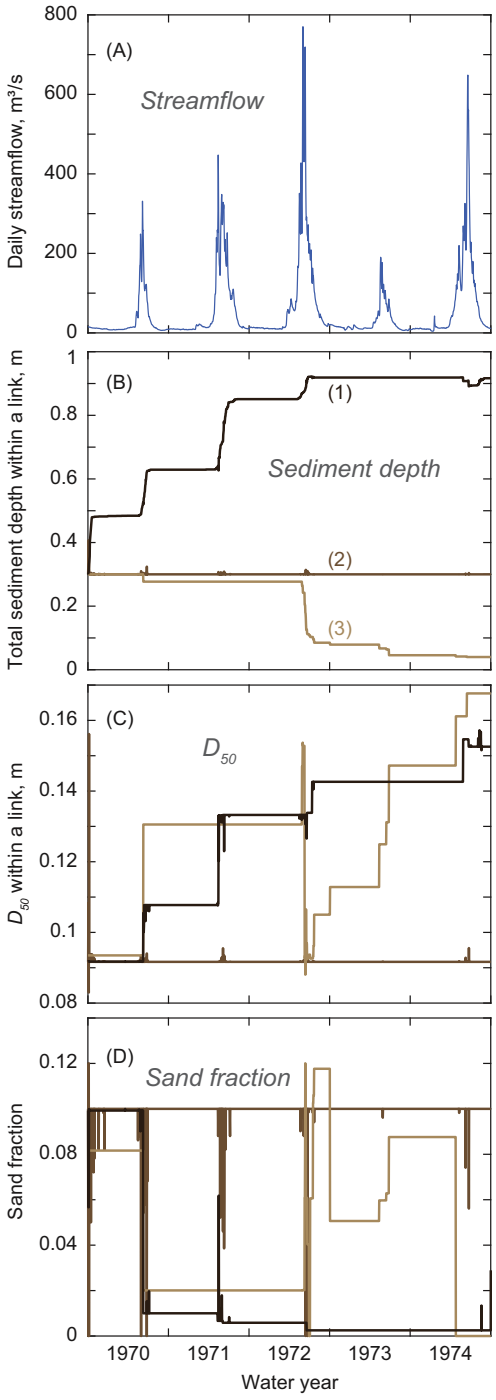

Fig. 2. Time series of flow and sedimentologic characteristics of three links. (A) Daily streamflow at the U.S. Geological Survey (USGS) gage (Methow River near Pateros, WA, 12449950). (B) Sediment depth, (C) D_{50}, and (D) sand fraction in three links located in Fig. 1. A water year begins on 1 Oct. of the previous year and ends on 30 Sept. of the listed year.

3.2.3. Sediment on the bed and input to the network

In the absence of grain size data for the entire basin, the available measured grain size distribution (measured near the middle of the network) was applied to the surface, subsurface, and sediment input grain size distributions for all links (Anchor QEA, 2011). This distribution had a D_{50} of roughly 0.09 m and was composed of 10% sand. The active layer thickness $L_{a,i,t}$ can be made to vary in space and time as a function of the characteristics of the sediment parcels within a link at a given time. For simplicity, a constant value for $L_{a,i,t}$ of 0.1 m was set for all links i and for all times t. Bed sediment thickness was computed using a

bed sediment porosity of 0.21 (see Czuba et al., 2017, for calculation of sediment thickness and see Wu and Wang, 2006, for calculation of porosity).

Surface and subsurface layers are composed entirely of sediment parcels where each parcel has its own volume and grain size. All sediment parcels were assigned a parcel volume $V_p = 10\ m^3$. The grain size of a sediment parcel was assigned a discrete value of $d_p \in \{2, 2.83, 5.66, 16.0, 45.3, 90.5, 181\ mm\}$, which represents the mean size within grain size bins bound by <2, 2, 4, 8, 32, 64, 128, and 256 mm. The grain size distribution of a link at any time is computed from the relative proportion of parcels of various sizes within that link. The measured grain size distributions guided how to populate the size distributions of the surface and subsurface layers and inputs. However, once initialized, parcels moved according to their own mobility relative to the other parcels within a link (via Wilcock and Crowe, Section 2.4.2). This allowed the grain size distribution to change within a link (and within surface and subsurface layers) through time, for instance, to represent armoring. The surface layer can only ever have a total parcel volume of at most $\chi_{i,t}$ (Eq. (3)). The surface and subsurface layers within each link were initialized with a total volume of parcels equivalent to the maximum value of $\chi_{i,t}$ in time for each link (see Eq. (2)) with relative proportions of grain sizes according to the measured grain size distribution. At time $t = 0$, sediment parcels with volume and grain size characteristics equivalent to that of the surface layer were input at each and every link. No other sediment inputs were added to the model simulation. Overall, >550,000 parcels were tracked within the system.

3.3. Overview of simulation and solution procedure

The model simulation began at time $t = 0$ and ran for 5 water years at a daily timestep (1 Oct. 1969–30 Sept. 1974). The presimulation procedure included (i) computing link attributes (see Section 3.2.1), (ii) assigning parameter values, (iii) specifying the flow series and computing $H_{i,t}$ and $B_{i,t}$ (see Section 3.2.2), and (iv) initializing sediment parcels in the subsurface and surface layers and inputting sediment parcels at time $t = 0$ (see Section 3.2.3). The initial conditions of the model included a network of channel links with unique slopes and the same grain size distribution for the surface and subsurface layers everywhere throughout the network. The boundary conditions of the model included (i) flow that varied in space, owing to hydraulic geometry scaling, and in time, owing to a daily flow series at a streamgage; and (ii) sediment parcel inputs with volume and grain size distribution equal to that present in the active layer of each link, delivered to each and every link at time $t = 0$. The solution procedure at each timestep included (i) computing the volume of sediment to move at transport capacity and placing this sediment in the active layer (see Section 2.3), (ii) updating slopes based on the volume of sediment in the storage layer (see Czuba et al., 2017), (iii) computing the sedimentological characteristics of the sediment parcels within the active/surface layer of each link (see Section 2.4.1), (iv) computing the transport time through a link of length ℓ_i, which can be converted to a virtual velocity given by $\ell_i/t_{p,i,t}$ for determining how far along the link that particular parcel moves within a given timestep (see Section 2.4.2), and (v) moving parcels to a new location within a link or into a downstream link based on its virtual velocity. This solution procedure is repeated for all timesteps and results in a Lagrangian tracking of sediment parcels as they move through links of the network. The collective parcels within a link affects the transport of those parcels through active/storage layer partitioning, slope adjustment based on parcels in storage, and size characteristics of the sediment mixture (via Wilcock and Crowe, 2003).

4. Results and discussion

At three different locations in the river network: (location 1) downstream near the basin outlet, (location 2) in the middle of the network, and (location 3) at a headwater link (see locations in Fig. 1), the simulated sedimentologic characteristics of sediment depth, D_{50}, and sand fraction are shown in Fig. 2. These simulated characteristics changed the most during high flows and remained constant during low flows. The magnitude of the yearly change in these characteristics was not readily predictable from the flow series alone because of nonlinearities in the transport of a sediment mixture and because of the ongoing adjustment of the model from the nonequilibrium initial conditions.

Near the basin outlet (location 1), the model simulated bed aggradation, a coarsening of the bed surface, and an export of sand. In the middle of the network (location 2), the model simulated a stable bed and grain size distribution, with an occasional decrease in sand fraction at high flows. In the headwaters (location 3), the model simulated bed degradation, a general coarsening of the bed, and a shift in the sediment distribution as coarser surface sediment was exported from the link allowing access to finer subsurface sediment (Fig. 2). This model behavior of downstream aggradation, mid-basin stability, and upstream degradation is not surprising given that the measured grain size distribution (measured near the middle of the network) was applied to the entire network. High in the basin, slopes were too steep for the input

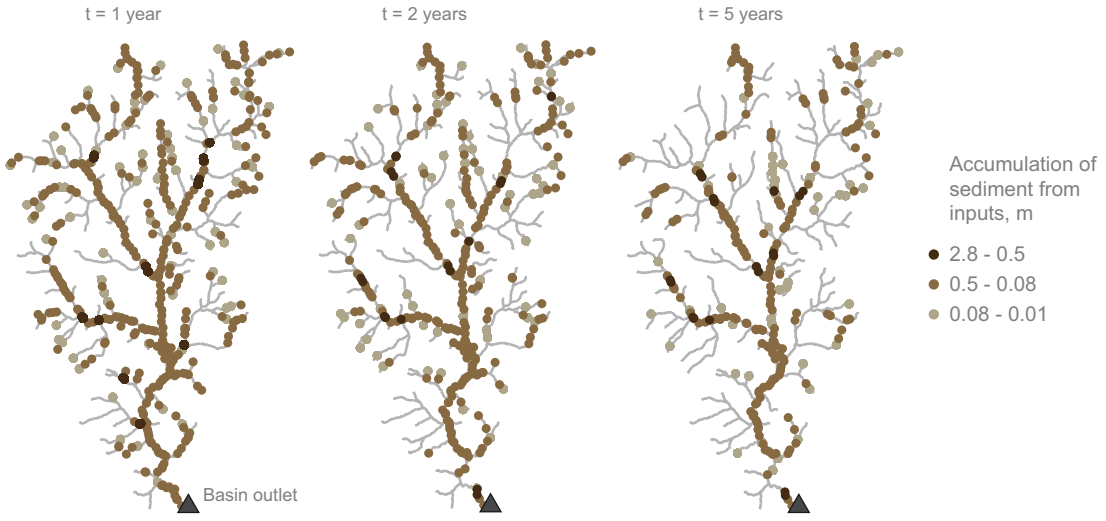

Fig. 3. Spatial distribution showing where all input sediment parcels with a grain size of 0.09 m have moved to after 1, 2, and 5 years of model simulation. This map does not show the parcels that initialized the surface and subsurface layers.

grain size distribution; and low in the basin, slopes were too low for the input grain size distribution — thus, the simulated channels were adjusting to this disequilibrium.

Every sediment parcel has a unique identifier and attributes. This information can be used to *tag* individual inputs or extract just the parcels with certain attributes. The locations of the input sediment parcels (not including the parcels used to initialize the surface and subsurface layers) with a grain size of 0.09 m are shown spatially throughout the network after 1, 2, and 5 years of model simulation in Fig. 3. Sediment transported rapidly out of steep headwater reaches and slowly through lowland reaches. Much of the downstream transport that occurred between years 2 and 5 years happened in year 3 with the highest streamflows (Fig. 2A). Each parcel in Fig. 3 is colored according to the local accumulation of sediment within that link, thus this information helps identify simulated aggradational hotspots throughout the network.

Maps such as those in Fig. 3 can be generated for each grain size group. Model simulations and maps of spatial results such as these were used to identify channel migration hotspots (Czuba and Foufoula-Georgiou, 2015) and *sediment bottlenecks*, i.e., local decreases in transport capacity that control sediment delivery to downstream reaches (Czuba et al., 2017; Schmitt et al., 2018). Grain-size-specific sediment bottlenecks could emerge in different locations on the network. The modeling framework presented herein is capable of identifying these locations in different river networks. However, exploring this possibility is beyond the scope of this paper.

The major limitation of this framework is that it has not been validated. Any serious applications of this framework will need data to support the predictions of the model. Such data might include a combination of bedload measurements at locations throughout the network, sediment load estimates from sediment accumulation in a downstream reservoir (if present), or long-term bed elevation changes at gages in the network. Additionally, predictions from this modeling framework could be compared to analogous 1D model simulations in select reaches.

This Lagrangian modeling framework allows for exploring complexities of mixed-size sediment transport in gravel-bedded river networks. Specifically, it allows for the investigation of how spatiotemporal sediment inputs are organized via transport in a river network. This sediment represents a mixture of sediment sizes that transport and interact (via Wilcock and Crowe, Section 2.4.2). Furthermore, this transport is punctuated by spatiotemporal streamflow forcing of intermittent sediment transporting flows. Simulating these dynamics at the scale of a river network is unique and this framework has opened up new avenues of inquiry. Upon further investigation and validation, the hope is that this work will allow for better understanding of watershed-scale dynamics in gravel-bedded rivers.

5. Summary

In this paper, a Lagrangian framework for exploring complexities of mixed-size sediment transport in gravel-bedded river networks was presented. The present model built off of previous network-based, bed-material sediment transport models, but its key advancements were in (i) allowing for a mixture of sediment sizes in the river network, (ii) incorporating a mixed-size sediment transport equation, and (iii) utilizing a daily flow hydrograph to drive intermittent transport. The model was applied to the roughly 4700 km^2 Methow River Basin in Washington State, USA, using simplified model inputs with the goal of illustrating the utility of the model for motivating future work.

Notation

A_i	upstream drainage area of link i [L^2]
b	an exponent
$B_{g,t}$	channel width at the gage at time t [L]
$B_{i,t}$	channel width of link i at time t [L]
$d_{i,t}$	mean size of bed surface sediment in link i at time t [L]
d_p	sediment parcel grain size [L]
$F_{p,i,t}$	fraction of parcel p in the active/surface layer of link i at time t
$F_{s,i,t}$	fraction of sand in the active/surface layer of link i at time t
g	acceleration due to gravity [LT^{-2}]
$H_{g,t}$	average flow depth at the gage at time t [L]
$H_{i,t}$	average flow depth in link i at time t [L]
i	link index
$L_{a,i,t}$	active layer thickness in link i at time t [L]
ℓ_i	length of link i [L]
p	sediment parcel index
$Q_{g,t}$	streamflow discharge at the gage at time t [L^3 T^{-1}]
R	submerged specific gravity of sediment
$S_{i,t}$	channel slope in link i at time t
t	time index [T]
$t_{p,i,t}$	travel time of sediment parcel p to move through link i at time t [T]
$V_{i,t}$	total parcel volume in link i at time t [L^3]
$V_{i,t}^{act}$	total parcel volume in the active/surface layer of link i at time t [L^3]
V_p	sediment parcel volume [L^3]
$W_{p,i,t}^*$	dimensionless sediment transport rate of parcel p in link i at time t
$\eta_{i,t}$	elevation of the bed at the upstream end of link i at time t [L]
ρ	density of water [ML^{-3}]
$\tau_{i,t}$	bed shear stress in link i at time t [ML^{-1} T^{-2}]
$\tau_{rp,i,t}$	reference shear stress for parcel p in link i at time t [ML^{-1} T^{-2}]
$\tau_{rm,i,t}$	reference shear stress for the mean size of the bed surface sediment in link i at time t [ML^{-1} T^{-2}]
$\chi_{i,t}$	volume of sediment in the active/surface layer of link i at transport capacity at time t [L^3]

Acknowledgements

This research did not receive any specific grant from funding agencies in the public, commercial, or not-for-profit sectors. The model is freely available from the corresponding author upon request. I thank the Editor (Richard A. Marston), Guest Editor (Peng Gao), and two anonymous reviewers for their comments that improved this manuscript.

References

Anchor QEA, 2011. 30 Percent Design Report Upper Middle Methow Reach WDFW Floodplain. Anchor QEA, Bellingham, WA 70 pp. http://methowsalmon.org/m2/docs/M2_30pct_Design_Report_WDFW_12-5-11.pdf, Accessed date: 24 January 2018.

Benda, L., Dunne, T., 1997a. Stochastic forcing of sediment routing and storage in channel networks. Water Resour. Res. 33 (12), 2865–2880. https://doi.org/10.1029/97WR02387.

Benda, L., Dunne, T., 1997b. Stochastic forcing of sediment supply to channel networks from landsliding and debris flow. Water Resour. Res. 33 (12), 2849–2863. https://doi.org/10.1029/97WR02388.

Benda, L., Andras, K., Miller, D., Bigelow, P., 2004. Confluence effects in rivers: Interactions of basin scale, network geometry, and disturbance regimes. Water Resour. Res. 40, W05402. https://doi.org/10.1029/2003WR002583.

Bureau of Reclamation, 2008. Methow Subbasin Geomorphic Assessment, Okanogan County, Washington. Bureau of Reclamation Technical Service Center, Denver, CO (844 pp).

Cui, Y., 2007. The Unified Gravel-Sand (TUGS) model: simulating sediment transport and gravel/sand grain size distributions in gravel-bedded rivers. Water Resour. Res. 43, W10436. https://doi.org/10.1029/2006WR005330.

Czuba, J.A., Foufoula-Georgiou, E., 2014. A network-based framework for identifying potential synchronizations and amplifications of sediment delivery in river basins. Water Resour. Res. 50 (5), 3826–3851. https://doi.org/10.1002/2013WR014227.

Czuba, J.A., Foufoula-Georgiou, E., 2015. Dynamic connectivity in a fluvial network for identifying hotspots of geomorphic change. Water Resour. Res. 51 (3), 1401–1421. https://doi.org/10.1002/2014WR016139.

Czuba, J.A., Foufoula-Georgiou, E., Gran, K.B., Belmont, P., Wilcock, P.R., 2017. Interplay between spatially-explicit sediment sourcing, hierarchical river-network structure, and in-channel bed-material sediment transport and storage dynamics. J. Geophys. Res. Earth Surf. 122 (5), 1090–1120. https://doi.org/10.1002/2016JF003965.

Frey, P., Church, M., 2011. Bedload: a granular phenomenon. Earth Surf. Process. Landf. 36 (1), 58–69. https://doi.org/10.1002/esp.2103.

Gran, K.G., Czuba, J.A., 2017. Sediment pulse evolution and the role of network structure. Geomorphology 277, 17–30. https://doi.org/10.1016/j.geomorph.2015.12.015.

Horizon Systems, 2018. NHDPlus Version 2. Horizon Systems Corporation, Herndon, VA Available at. http://www.horizon-systems.com/NHDPlus/NHDPlusV2_home.php, Accessed date: 30 January 2018.

Jacobson, R.B., Gran, K.B., 1999. Gravel sediment routing from widespread, low- intensity landscape disturbance, Current River Basin, Missouri. Earth Surf. Process. Landf. 24 (10), 897–917. https://doi.org/10.1002/(SICI)1096-9837(199909)24:10<897::AID-ESP18>3.0.CO;2-6.

Lauer, J.W., Viparelli, E., Piégay, H., 2016. Morphodynamics and sediment transport in 1-D (MAST-1D): 1-D sediment transport that includes exchange with an off-channel sediment reservoir. Adv. Water Resour. 93 (A), 135–149. https://doi.org/10.1016/j.advwatres.2016.01.012.

Leopold, L.B., Maddock Jr., T., 1953. The hydraulic geometry of stream channels and some physiographic implications. U.S. Geological Survey Professional Paper. Vol. 252. U.S. Geological Survey, Washington, D.C. (57 pp).

Mastin, M., 2015. Simulated runoff at many stream locations in the Methow River Basin, Washington. U.S. Geological Survey Open-File Report 2015-1011. U.S. Geological Survey, Reston, VA https://doi.org/10.3133/ofr20151011 (22 pp).

McKay, L., Bondelid, T., Dewald, T., et al., 2012. NHDPlus Version 2: User Guide. U.S. Environmental Protection Agency, Washington, D.C. ftp://ftp.horizon-systems.com/NHDPlus/NHDPlusV21/Documentation/NHDPlusV2_User_Guide.pdf, Accessed date: 30 January 2018.

Ockelford, A.-M., Haynes, H., 2013. The impact of stress history on bed structure. Earth Surf. Process. Landf. 38 (7), 717–727. https://doi.org/10.1002/esp.3348.

Park, C.C., 1977. World-wide variations in hydraulic geometry exponents of stream channels: an analysis and some observations. J. Hydrol. 33, 133–146. https://doi.org/10.1016/0022-1694(77)90103-2.

Parker, G., 2008. Transport of gravel and sediment mixtures. In: Garcia, M.H. (Ed.), Sedimentation Engineering: Processes, Measurements, Modeling, and Practice. ASCE manuals and reports on engineering practice 110. ASCE, Reston, VA, pp. 165–251.

Rice, S.P., 2017. Tributary connectivity, confluence aggradation, and network biodiversity. Geomorphology 277, 6–16. https://doi.org/10.1016/j.geomorph.2016.03.027.

Schmitt, R.J.P., Bizzi, S., Castelletti, A., 2016. Tracking multiple sediment cascades at the river network scale identifies controls and emerging patterns of sediment connectivity. Water Resour. Res. 52, 3941–3965. https://doi.org/10.1002/2015WR018097.

Schmitt, R.J.P., Bizzi, S., Castelletti, A.F., Kondolf, G.M., 2018. Stochastic modeling of sediment connectivity for reconstructing sand fluxes and origins in the unmonitored Se Kong, Se San, and Sre Pok tributaries of the Mekong River. J. Geophys. Res. Earth Surf. 123 (1), 2–25. https://doi.org/10.1002/2016JF004105.

Sklar, L.S., Riebe, C.S., Marshall, J.A., Ganetti, J., Leclere, S., Lukens, C.L., Merces, V., 2017. The problem of predicting the size distribution of sediment supplied by hillslopes to rivers. Geomorphology 277, 31–49. https://doi.org/10.1016/j.geomorph.2016.05.005.

U.S. Geological Survey (USGS), 2018. USGS 12449950 Methow River near Pateros, WA. https://waterdata.usgs.gov/nwis/inventory/?site_no=12449950, Accessed date: 31 January 2018.

Walley, Y., Tunnicliffe, J., Brierley, G., 2018. The influence of network structure upon sediment routing in two disturbed catchments, East Cape, New Zealand. Geomorphology 307, 38–49. https://doi.org/10.1016/j.geomorph.2017.10.029.

Wilcock, P.R., Crowe, J.C., 2003. Surface-based transport model for mixed-size sediment. J. Hydraul. Eng. 129 (2), 120–128. https://doi.org/10.1061/(ASCE)0733-9429(2003)129:2(120).

Wilkinson, S.N., Prosser, I.P., Hughes, A.O., 2006. Predicting the distribution of bed material accumulation using river network sediment budgets. Water Resour. Res. 42, W10419. https://doi.org/10.1029/2006WR004958.

Wu, W., Wang, S., 2006. Formulas for sediment porosity and settling velocity. J. Hydraul. Eng. 132, 858–862. https://doi.org/10.1061/(ASCE)0733-9429(2006)132:8(858).

Zanardo, S., Zaliapin, I., Foufoula-Georgiou, E., 2013. Are American rivers Tokunaga self-similar? New results on fluvial network topology and its climatic dependence. J. Geophys. Res. Earth Surf. 118, 166–183. https://doi.org/10.1029/2012JF002392.